Stepping Motor Drive for Precise Positioning Applications

Mikho R. Mikhov[1], Panayot S. Nakov[2]

Abstract – **The performance of a hybrid stepping motor drive system developed for precise position mechanisms is discussed in this paper. Load influence on motion trajectories is shown and the respective speed profiles are derived. The drive behavior in microstepping operation mode is analyzed. The results obtained can be used in the design of such types of positioning drive systems.**

Keywords – **Stepping motor drive, Position control.**

I. Introduction

Stepping motors have a number of advantages, such as: position accuracy, wide speed range, simple and robust construction, ability to operate in open-loop drive systems, and easy compatibility with microprocessor controllers [1], [2].

Hybrid stepping motors combine the best characteristics of both variable reluctance and permanent magnet motors. They are appropriate in applications requiring small step length and high torque within restricted working space.

The microstepping control can ensure some following additional advantages such as: higher position accuracy and resolution, vibrations and noise reduction, as well as elimination or simplification of the gearboxes [3], [4], [6].

The performance of a hybrid stepping motor drive system developed for precise position applications is presented in this paper. Load influence on motion trajectories is shown and the respective acceleration and deceleration speed profiles are derived. The drive system behavior in microstepping control mode is analyzed to determine the necessary micro-step length in compliance with the desired accuracy.

II. Features of the Used Stepping Motor

The magnetic circuit of hybrid stepping motor is excited by a combination of windings and permanent magnet. The windings are placed on the stator while the permanent magnet is mounted on the rotor. The rotor comprises a pair of laminated toothed cylinders as shown in Fig. 1. The teeth on the two sections are misaligned with respect to each other by half tooth pitch. When the windings are unexcited the magnet flux produces a small detent torque, which retains the rotor at the step position.

The following assumptions have been made [5]:

- the magnetic coupling between the phases is neglected, as it is slight in hybrid step motors;

- the variation of inductance with position is not taken into account because it is negligible for permanent magnet stepping motors;

- the effect of saturation at high phase currents is ignored. The saturation influence reduces in high-speed regions where currents are limited because of the back electromotive force voltage.

The electric and mechanical equations representing the used two-phase hybrid stepping motor are as follows:

$$v_a = L\frac{di_a}{dt} + Ri_a - K_t\omega\sin(p\theta); \tag{1}$$

$$v_b = L\frac{di_b}{dt} + Ri_b + K_t\omega\cos(p\theta); \tag{2}$$

$$T = -K_t i_a \sin(p\theta) + K_t i_b \cos(p\theta); \tag{3}$$

$$\omega = \frac{d\theta}{dt}; \tag{4}$$

$$T = J\frac{d\omega}{dt} + T_l, \tag{5}$$

where:

v_a and v_b are phase voltages;
i_a and i_b – phase currents;
ω – angular velocity;
θ – rotor position;
T – motor torque;
K_t – torque constant;
R – winding resistance;
L – winding inductance;
p – number of the rotor teeth;
J – total inertia referred to the motor shaft;
T_l – load torque.

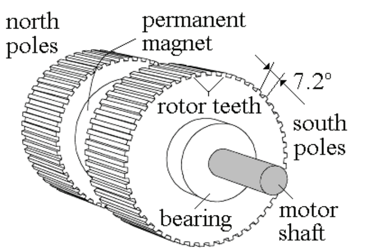

Fig. 1. The rotor of the hybrid step motor.

The simplified block diagram of the developed position drive system is shown in Fig. 2, where the notations are as follows: KB – keyboard; C – controller; PC – power conver-

[1]Mikho R. Mikhov is with the Faculty of Automatics, Technical University of Sofia, 8 Kliment Ohridski Str., 1797 Sofia, Bulgaria, E-mail: mikhov@tu-sofia.bg

[2]Panyot S. Nakov is with the Faculty of Automatics, Technical University of Sofia, 8 Kliment Ohridski Str., 1797 Sofia, Bulgaria, E-mail: p.nakov@abv.bg

ter; DP – display; SU – supply unit; SM – hybrid step motor; PE – position encoder; L – load applied to the motor shaft.

III. MOTION TRAJECTORY FORMATION

There are two operating regions of the stepping motor, namely start/stop and slew ones (fig. 3). They are defined by pull-in and pull-out torque curves, respectively. To operate the motor at higher speeds, it is necessary to start at a frequency within the first area and then accelerate the motor into the second range. When stopping the motor, it must be decelerated back into the start/stop region before the clock pulses are terminated. Otherwise, synchronization in rotor positioning will be lost.

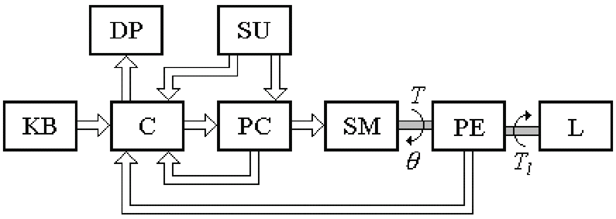

Fig. 2. Simplified block diagram of the position drive system.

Acceleration and deceleration of stepping electric drives depend on both load torque and total inertia referred to the motor shaft. To ensure maximum speed of the position system, control should be applied in accordance with the pull-out curve.

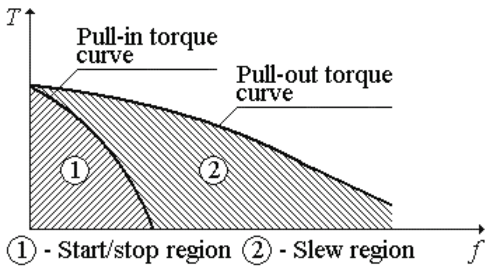

Fig. 3. Operating regions of the stepping motor.

The angular velocity and rotor position can be expressed through its mechanical step, as follows:

$$\omega = \alpha f \, ; \tag{6}$$

$$\theta_{M} = \alpha N \, , \tag{7}$$

where:

f is frequency of the clock pulses;

N – number of the steps.

The mechanical step of the motor used can be determined through the next equation:

$$\alpha = 2\pi/4p \tag{8}$$

Reading Eqs. (6) and (7), to achieve the desired trajectory $\omega(\theta)$, the respective $f(N)$ can be programmed. Fig. 4 shows such a motion trajectory, during execution of an assigned position cycle. The following notations have been used: f_r – reference frequency, corresponding to the desired angular velocity; N_r - reference number of steps, congruent to the desired transposition distance.

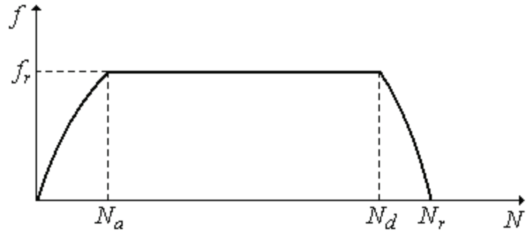

Fig. 4. Motion trajectory for a reference position cycle.

The speed profile has three sectors, namely:

- acceleration $(df/dt > 0)$;
- constant speed $(f = f_r = \text{const})$;
- deceleration $(df/dt < 0)$.

Taking into consideration Eq. (6), Eq. (5) becomes as follows:

$$J\alpha \frac{df}{dt} + T_l = T(f) \tag{9}$$

The acceleration / frequency dependence for the starting regime is obtained from Eq. (9):

$$\left[\frac{df}{dt}(f)\right]_a = \dot{f}_a(f) = \frac{T(f) - T_l}{J\alpha}\,. \tag{10}$$

The stepping rate as a function of time during acceleration can be derived after integration of this equation:

$$t = \int_{f_0}^{f} \frac{df}{\dot{f}_a(f)} \rightarrow [f(t)]_a \tag{11}$$

where f_0 is the initial frequency, from which acceleration proceeds.

The corresponding relation between the impulse frequency and step number can be obtained from the following equation:

$$N = \int_{f_0}^{f} \frac{f}{\dot{f}_a(f)} df \rightarrow [f(N)]_a\,. \tag{12}$$

Deceleration, as a function of frequency can be determined in an analogical way:

$$\left[\frac{df}{dt}(f)\right]_d = \dot{f}_d(f) = -\frac{T(f) + T_l}{J\alpha}\,, \tag{13}$$

Applying Eq. (13) for the deceleration process, these relations have been derived:

$$t = \int_{f_r}^{f} \frac{df}{\dot{f}_d(f)} \to [f(t)]_d \; ; \tag{14}$$

$$N = \int_{f_r}^{f} \frac{f}{\dot{f}_d(f)} df \to [f(N)]_d \; . \tag{15}$$

Motion trajectory formation is carried out in the following sequence:

1. The pull-out torque curve $T(f)$ should be specified experimentally.
2. Next, an appropriate approximation for the obtained curve is carried out.
3. In compliance with Eqs. (10) and (13) the $\dot{f}_a(f)$ and $\dot{f}_d(f)$ relationships are determined.
4. Through Eqs. (12) and (15) acceleration and deceleration profiles $[f(N)]_a$ and $[f(N)]_d$ are obtained.
5. The respective motion trajectory is programmed for the desired position cycle $f(N)$.

IV. Determination of the Micro-Step Length

To improve the position accuracy in the developed position system microstepping control has been applied. In this operating mode the full step length is divided electronically into small increments of rotor motion:

$$\alpha_\mu = \alpha / n \, , \tag{16}$$

where:
n is the number of micro-steps;
α_μ – the angular displacement of each micro-step.

Subdivision of the basic motor step is possible by proportioning the phase currents in the two windings (Fig. 5). Current magnitudes vary and the number of current levels depends on the desired micro-step size.

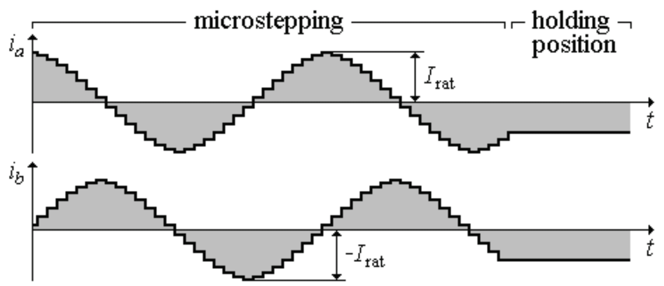

Fig. 5. Current waveforms in microstepping operation.

Air gap flux is proportional to the vector sum of the winding currents, in the resultant vector direction. To achieve a required rotating flux, the phase currents' magnitudes are calculated as follows:

$$i_a(N_i) = I_{\text{rat}} \cos(i a_\mu); \tag{17}$$

$$i_b(N_i) = I_{\text{rat}} \sin(i a_\mu), \tag{18}$$

where:
I_{rat} is the rated phase current;
N_i – the number of current levels;
$i = 0, 1, 2, ..., 4n - 1$.

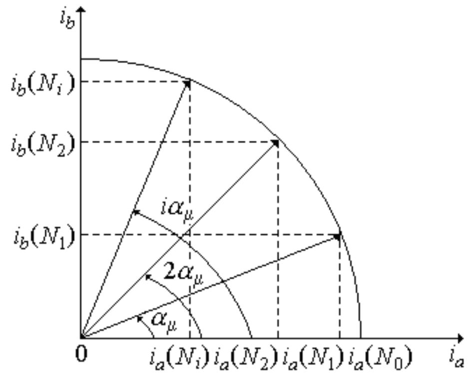

Fig. 6. Vector diagram for microstepping control.

The respective current vector diagram is represented in Fig. 6. The resultant stator current represents the phase currents vector sum:

$$I = \sqrt{[I_{\text{rat}} \cos(i\alpha_\mu)]^2 + [I_{\text{rat}} \sin(i\alpha_\mu)]^2} = I_{\text{rat}} \, . \tag{19}$$

Eq. (19) shows that the resultant current remains uniform and equal to the rated value. Therefore, by correct combination of phase current levels it is possible to obtain constant resultant current and smooth movement of the stepping motor shaft.

For conventional operation modes the equilibrium positions are defined by alignment of the stator and rotor teeth and they are independent of the current levels. However, the micro-step positions are critically dependent on current levels in the phase windings. Therefore, there is a need for closed-loop current control to provide the respective correct phase current levels.

Tuning of the microprocessor control system is carried out in the following sequence:

1. The appropriate micro-step α_μ is calculated in accordance with the desired position resolution ΔS_d:

$$\alpha_\mu \le \Delta S_d / K_g \, , \tag{20}$$

where: K_g [m/rad] is the gear coefficient.

2. The number of micro-steps n is defined on the basis of the α_μ value.
3. The necessary phase current levels are calculated in compliance with Eq. (17) and Eq. (18).
4. A respective lookup table for the microstepping mode of

operation is compiled.

For the case under consideration the parameters are as follows:

- desired position resolution $\Delta S_d = 10\,\mu\text{m}$;
- gear coefficient $K_g = 10$ mm/rev. $\approx 1.6\text{x}10^{-3}$ m/rad.
- full motor step $\alpha = 1.8° \approx 0.0314$ rad;
- number of micro-steps per one full motor step $n = 8$;
- micro-step $\alpha_\mu = \alpha/8 \approx 0.00393$ rad;
- provided position resolution $\Delta S_p = 6.25\,\mu\text{m} < \Delta S_d$.

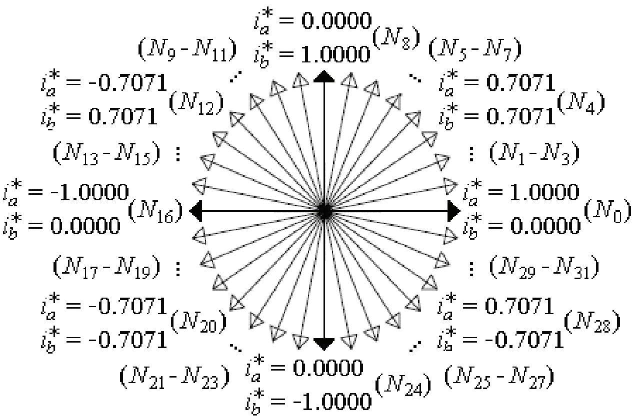

Fig. 7. Current levels when one full step is divided into 8 sub-steps.

The current levels calculated for obtaining constant motor torque are given in Fig. 7. One full electrical step is divided into eight micro-steps, and the currents are represented in relative units:

$$i_a^* = i_a / I_{\text{rat}} \; ; \tag{21}$$

$$i_b^* = i_b / I_{\text{rat}} \; . \tag{22}$$

Fig. 8 shows the position response in full step operation mode ($\alpha = 1.8° \approx 0.0314$ rad), when the two phases are excited simultaneously.

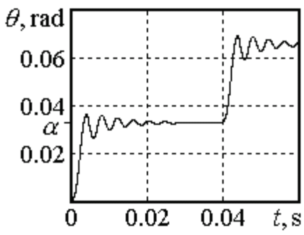

Fig. 8. Position response in full step operation mode.

The applied microstepping control is illustrated by Fig. 9. One full motor step is divided into eight sub-steps and the resolution in this case is 1600 micro-steps per revolution ($\alpha_\mu = \alpha/8 \approx 0.00393$ rad).

VI. CONCLUSION

A hybrid stepping motor drive system developed for precise position mechanisms has been studied, aiming at improvement of its performance.

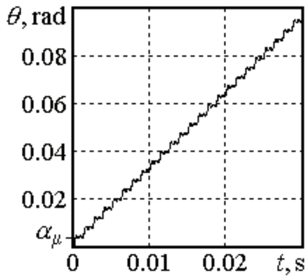

Fig. 9. Position response in microstepping operation mode when one full step is divided into 8 sub-steps.

Theoretical and experimental research has been carried out for two-phase hybrid stepping motors with basic parameters as follows:

- rated voltage $V_{\text{rat}} = 5$ V;
- rated phase current $I_{\text{rat}} = 1$ A;
- number of the rotor teeth $p = 50$;
- full motor step $\alpha = 1.8°$.

Load influence on motion trajectories has been analyzed resulting into derivation of the respective acceleration and deceleration speed profiles.

Investigations on the drive system behavior in microstepping operation mode show, that the applied method for control allows any sub-step length. However there is a practical limit on how small micro-steps can become until the rotor and its mechanical load cease to react adequately. Limitations can be induced by the following factors:

- static friction in the system;
- non-sinusoidal character of the torque versus rotor position curves;
- current quantization resolution.

The stepping motor drive system described above improves the positioning resolution, reduces shaft vibrations and ensures maximum torque at both low and high speeds. It is particularly suitable for precise applications where the required step resolution is higher than that, provided by conventional operation modes.

The results obtained can be used in the design of such types of position drive systems.

REFERENCES

[1] P. P. Acarnley, *Stepping motors: a guide to theory and practice*, London, IEE, 2002.

[2] T. Kenjo, *Stepping motors and their microprocessor controls*, Oxford, Clarendon, 1984.

[3] M. A. Freitas, D. A. Andrade, T. T. Borges, H. R. Azevedo, “Driving the step motor with controlled phase currents”, *Proceedings of the PEDES*, pp. 493-498, Perth, Australia, 1998.

[4] C. Park, S. Kim, H. Ahn, S. Park, “Characteristic improvement of 5 phase step motor by using micro-step driver in X-Y axis soldering machine”, *Proceedings of the ICPE*, pp. 97-100, Seoul, Korea, 1998.

[5] M. R. Mikhov, “Modeling and investigation of a step motor drive with microstepping control”, *Proceedings of the ICAI*, pp. 135-138, Sofia, Bulgaria, 2005.

[6] M. R. Mikhov, P. S. Nakov, “A hybrid step motor drive system with high positioning accuracy”, *Proceedings of the EDS*, pp. 59-64, Brno, Czech Republic, 2005.